

Measurement of the Positive Muon Anomalous Magnetic Moment to 0.7 ppm

G. W. Bennett,² B. Bousquet,⁹ H. N. Brown,² G. Bunce,² R. M. Carey,¹ P. Cushman,⁹ G. T. Danby,² P. T. Debevec,⁷ M. Deile,¹¹ H. Deng,¹¹ W. Deninger,⁷ S. K. Dhawan,¹¹ V. P. Druzhinin,³ L. Duong,⁹ E. Efstathiadis,¹ F. J. M. Farley,¹¹ G. V. Fedotovich,³ S. Giron,⁹ F. E. Gray,⁷ D. Grigoriev,³ M. Grosse-Perdekamp,¹¹ A. Grossmann,⁶ M. F. Hare,¹ D. W. Hertzog,⁷ X. Huang,¹ V. W. Hughes,¹¹ M. Iwasaki,¹⁰ K. Jungmann,⁵ D. Kawayall,¹¹ B. I. Khazin,³ J. Kindem,⁹ F. Krienen,¹ I. Kronkvist,⁹ A. Lam,¹ R. Larsen,² Y. Y. Lee,² I. Logashenko,^{1,3} R. McNabb,⁹ W. Meng,² J. Mi,² J. P. Miller,¹ W. M. Morse,² D. Nikas,² C. J. G. Onderwater,⁷ Y. Orlov,⁴ C. S. Özben,² J. M. Paley,¹ Q. Peng,¹ C. C. Polly,⁷ J. Pretz,¹¹ R. Prigl,² G. zu Putlitz,⁶ T. Qian,⁹ S. I. Redin,^{3,11} O. Rind,¹ B. L. Roberts,¹ N. Ryskulov,³ P. Shagin,⁹ Y. K. Semertzidis,² Yu. M. Shatunov,³ E. P. Sichtermann,¹¹ E. Solodov,³ M. Sossong,⁷ A. Steinmetz,¹¹ L. R. Sulak,¹ A. Trofimov,¹ D. Urner,⁷ P. von Walter,⁶ D. Warburton,² and A. Yamamoto⁸

(Muon ($g - 2$) Collaboration)

¹*Department of Physics, Boston University, Boston, Massachusetts 02215*

²*Brookhaven National Laboratory, Upton, New York 11973*

³*Budker Institute of Nuclear Physics, Novosibirsk, Russia*

⁴*Newman Laboratory, Cornell University, Ithaca, New York 14853*

⁵*Kernfysisch Versneller Instituut, Rijksuniversiteit Groningen, NL 9747 AA Groningen, The Netherlands*

⁶*Physikalisches Institut der Universität Heidelberg, 69120 Heidelberg, Germany*

⁷*Department of Physics, University of Illinois at Urbana-Champaign, Urbana-Champaign, Illinois 61801*

⁸*KEK, High Energy Accelerator Research Organization, Tsukuba, Ibaraki 305-0801, Japan*

⁹*Department of Physics, University of Minnesota, Minneapolis, Minnesota 55455*

¹⁰*Tokyo Institute of Technology, Tokyo, Japan*

¹¹*Department of Physics, Yale University, New Haven, Connecticut 06520*

(Received 31 July 2002; published 20 August 2002; publisher error corrected 23 August 2002)

A higher precision measurement of the anomalous g value, $a_\mu = (g - 2)/2$, for the positive muon has been made at the Brookhaven Alternating Gradient Synchrotron, based on data collected in the year 2000. The result $a_{\mu^+} = 11\,659\,204(7)(5) \times 10^{-10}$ (0.7 ppm) is in good agreement with previous measurements and has an error about one-half that of the combined previous data. The present world average experimental value is $a_\mu(\text{expt}) = 11\,659\,203(8) \times 10^{-10}$ (0.7 ppm).

DOI: 10.1103/PhysRevLett.89.101804

PACS numbers: 13.40.Em, 12.15.Lk, 14.60.Ef

The study of magnetic moments has played an important role in our understanding of subatomic physics. Precision measurements of the electron anomalous magnetic moment, together with those of the hyperfine structure of hydrogen and the Lamb shift, stimulated the development of modern quantum electrodynamics and have since provided stringent tests of this theory. In this Letter we report a new measurement of the anomalous magnetic moment of the positive muon, $a_\mu = (g - 2)/2$, with a relative precision of 0.7 parts per million (ppm), nearly 2 times better than our previous work [1–3]. This measurement comes from data collected in the year 2000. At this level, a_μ is sensitive to QED, weak, and hadronic virtual loops and provides an important constraint on extensions to the standard model.

The principle of the experiment and previous results have been given in earlier publications [1–3]. Also, detailed descriptions of the ($g - 2$) superconducting inflector magnet, storage ring magnet, fast kicker, NMR system, and calorimeters have been published [4].

The quantity a_μ is determined from

$$a_\mu = \frac{\omega_a}{(e/m_\mu c)\langle B \rangle}. \quad (1)$$

The magnetic field $\langle B \rangle$ weighted over the muon beam distribution is measured by proton NMR. The difference frequency ω_a between the muon spin precession and orbital angular frequencies is determined by counting the number $N(t)$ of decay positrons with energies larger than an energy threshold,

$$N(t) = N_0(E)e^{-t/(\gamma\tau)}\{1 + A(E)\sin[\omega_a t + \phi_a(E)]\}. \quad (2)$$

The normalization N_0 , asymmetry A , and phase ϕ_a vary with the chosen threshold. The time dilated lifetime is $\gamma\tau \approx 64.4 \mu\text{s}$. For muons with $\gamma = 29.3$, the angular difference frequency ω_a is not affected by electrostatic focusing fields in the ring.

New aspects of the 2000 data-taking period include the operation of the Alternating Gradient Synchrotron (AGS)

with 12 beam bunches, contributing to a fourfold increase in data collected as compared to 1999; a new superconducting inflector magnet, which improved the field homogeneity in the muon storage region; the installation and operation of a sweeper magnet in the beam line, which reduced AGS background; and additional muon loss detectors, which enable an improved determination of the time dependence of muon losses. Most other experimental aspects of the data taking in 2000 were the same as in 1998 and 1999.

The magnetic field value was obtained from NMR measurements of the free proton resonance frequency. A trolley with 17 NMR probes was used to measure the field throughout the muon storage ring, typically every 3 d. The trolley probes were calibrated to an accuracy of 0.15 ppm with respect to a standard spherical H₂O probe, which has an absolute calibration known to 0.05 ppm. The probes were intercalibrated during the data-taking period using a single, movable probe plunged into the storage region. Interpolation of the magnetic field between trolley measurements was based on the continual readings of about 150 fixed NMR probes distributed around the ring in the top and bottom walls of the vacuum chamber. Figure 1 shows a magnetic field profile averaged over azimuth. The improved field homogeneity obtained with the new inflector relaxes the demands on the knowledge of the muon beam distribution.

The field $\langle B \rangle$ averaged over the muon beam distribution in space and time was obtained from two complete and largely independent analyses, whose results were found to agree to within 0.05 ppm. Its final value is expressed in terms of the free proton resonance frequency and is given by $\omega_p/(2\pi) = 61\,791\,595(15)$ Hz (0.2 ppm). Table I lists the uncertainties.

The frequency ω_a was obtained from the time distribution of decay positron counts. The positrons were detected with 24 lead/scintillating fiber calorimeters on the inside of

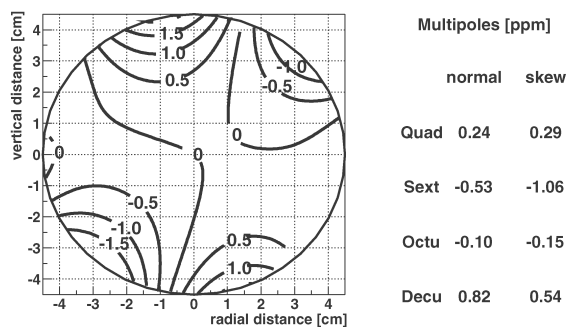


FIG. 1. A two-dimensional multipole expansion of the field averaged over azimuth from 1 out of 22 trolley measurements. Half ppm contours with respect to a central azimuthal average field $B_0 = 1.451\,274$ T are shown. The multipole amplitudes relative to B_0 are given at the beam aperture, which has a radius of 4.5 cm and is indicated by the circle.

the storage ring, whose photomultiplier signals had a typical FWHM of 5 ns. The signals were recorded with 400 MHz, 8-bit waveform digitizers (WFD). Pulses above a preset energy threshold of about 1 GeV triggered the WFD to record at least 16 samples (40 ns). Pulses with energies below the hardware threshold were recorded if they appeared within the sampling window around a trigger pulse. The positron arrival times and energies were reconstructed off-line from the WFD recordings using two independent implementations of our pulse reconstruction algorithm.

The large positron sample and 30% higher instantaneous count rates than in 1999 required careful consideration of distortions to the spectrum in Eq. (2). As in the analysis of our 1999 data, we have considered (1) positron pulses overlapping in time (pileup), (2) coherent betatron oscillations, (3) beam debunching, (4) muon losses, and (5) detector gain and time instability.

(1) Pileup of positron signals distorts the time spectrum because of misidentification of the number, energies, and times of the positrons. The pileup spectrum can be constructed from the data using the extended pulse sampling by the WFD described above, and can effectively be subtracted from the data prior to fitting [3].

(2) As in earlier data-taking periods, the weak focusing storage ring was operated with a field index $n = 0.137$, well away from beam and spin resonances. The phase space for betatron oscillations defined by the acceptance of the storage ring was not filled, which resulted in coherent betatron oscillations (CBO)—betatron oscillations of the beam as a whole. Since the acceptance of a calorimeter varies with the radial muon decay position in the storage ring and the momentum of the produced decay positron, the observed positron time and energy spectra are modulated with the CBO frequencies. The most important modulation is the horizontal one with frequency $\omega_{\text{CBO,h}} = (1 - \sqrt{1 - n})\omega_c = 2\pi \times 466$ kHz, where ω_c is the cyclotron frequency. At injection time, this modulation affects the terms N_0 , A , and ϕ_a in Eq. (2) at the level of 1%, 0.1%, and 1 mrad, respectively.

TABLE I. Systematic uncertainties for the ω_p analysis.

Source of errors	Size (ppm)
Absolute calibration of standard probe	0.05
Calibration of trolley probe	0.15
Trolley measurements of B_0	0.10
Interpolation with fixed probes	0.10
Uncertainty from muon distribution	0.03
Others ^a	0.10
Total systematic error on ω_p	0.24

^aHigher multipoles, trolley temperature and voltage response, eddy currents from the kickers, and time-varying stray fields.

For $n = 0.137$, the frequency $\omega_{\text{CBO,h}}$ is approximately twice as large as ω_a and, hence, the interference frequency $\omega_{\text{CBO,h}} - \omega_a$ is close to ω_a . Modulations of the asymmetry and phase with frequencies $\omega_{\text{CBO,h}} \approx 2 \times \omega_a$ may, unlike the modulation of observed counts, manifest themselves as sizable, artificial shifts in the fitted frequency value ω_a , when not taken into account in the function fitted to the data. These shifts are as large as 4 ppm for individual calorimeter time spectra and mostly cancel in the summed spectra owing to the circular symmetry of the experiment design.

The existence of CBO and their effect on the positron time spectra can be seen from Fig. 2, showing the Fourier amplitudes of residuals from fits to the data based only on muon decay and spin precession [Eq. (2)]. The Fourier amplitudes at the interference frequencies $\omega_{\text{CBO,h}} \pm \omega_a$ differ by about 20% because of the aforementioned modulation of the observed phase. The characteristic CBO decay times were $\sim 100 \mu\text{s}$.

(3) The injection of the beam in narrow bunches into the storage ring resulted in a strong modulation of the initial part of the positron time spectrum with the 149.2 ns cyclotron period. This effect was removed from the analyses by uniformly randomizing the recorded start time for each beam pulse over one cyclotron period.

(4) Losses of muons during the data collection were minimized by controlled scraping [2] of the beam before the data collection started. The time dependence of small, residual losses was determined by forming triple coincidences from scintillating detectors mounted to the face of

three adjacent calorimeters. Corrections were made for accidental coincidences and proton background. The time spectrum of lost muons was measured, up to a normalization, at five locations in the storage ring.

(5) Average calorimeter timing shifts were determined with a pulsed UV laser system to be typically smaller than 4 ps over the first 200 μs of data taking. Detector gain changes are determined from the average observed positron energy as a function of time after beam injection. From 50 μs on, 5 μs after the last of the calorimeters was gated on in 2000, the gains of all but two of the calorimeters were stable to within 0.2% over the ten dilated muon lifetimes of data collection.

The event sample collected in the year 2000 amounts, after data selection, to 4×10^9 positrons with energies greater than 2 GeV in the time region 50 to 600 μs following muon injection into the storage ring. A statistical uncertainty in the fitted frequency ω_a of about 0.7 ppm results. To assess systematic uncertainties to an adequate precision, distortions of the decay positron spectrum in Eq. (2) have been studied in the full range of observed energies. In addition, the time spectrum for positron energies exceeding 2 GeV has been studied, as well as two representations of the time spectra that suppress periodic distortions with frequency $\omega_{\text{CBO,h}}$ and slow distortions, respectively. In total, four independent and complete analyses of ω_a were performed.

In the first analysis the data were fitted in 0.2 GeV energy intervals in the range 1.4–3.2 GeV for each detector separately. This results in 198 independent fits. The pileup contribution to each spectrum was determined from the WFD recordings using a variant of the technique used before. For each energy interval and each calorimeter station, pileup was statistically constructed and fitted to an appropriate functional form. The resulting parameters were then incorporated into the fitting function used to describe the positron time spectra. Horizontal CBO were incorporated in the function fitted to the data through modulation of the observed number of counts, asymmetry, and phase. The function fitted to the calorimeter data in each energy interval is given by

$$N(t) = N_0(t; E)e^{-t/(\gamma\tau)}\{1 + A(t; E)\sin[\omega_a t + \phi_a(t; E)]\}, \quad (3)$$

in which the time dependences of N_0 , A , and ϕ_a are all modulated as $\sim 1 + \mathcal{A}_i(t)\sin(\omega_{\text{CBO,h}}t + \phi_i)$, where i stands for any of the three separate modulations of N_0 , A , and ϕ_a . The modulation amplitudes were determined empirically from the data and follow primarily an exponential with a characteristic decay time of approximately 100 μs . Muon losses were constrained to the shape of the measured losses. The spectrum described by Eq. (3) is multiplied by a time-dependent factor which accounts for these losses. Fit start times for each calorimeter station and energy interval were chosen at times after which the quality of

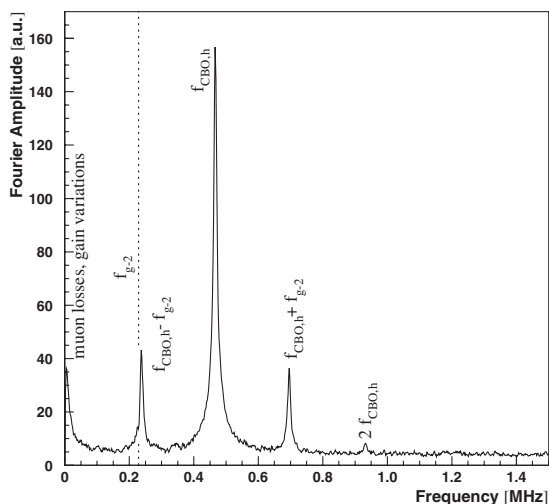


FIG. 2. CBO in the $g - 2$ time spectra. The Fourier spectrum was obtained from residuals from a fit based on muon decay and spin precession [Eq. (2)] alone. The horizontal modulation was at $\omega_{\text{CBO,h}}/(2\pi) = 466 \text{ kHz}$ in the year 2000, so that the interference frequency $\omega_{\text{CBO,h}} - \omega_a$ is numerically close to ω_a , as indicated. The frequency ω_a is determined from fits that take CBO into account.

fit has become constant. Slowly vanishing distortions of the exponential, due to imperfectly corrected energy scale variations, pileup, or muon losses, are thereby removed.

In the second analysis the time spectrum of all positrons with energies larger than 2 GeV and arrival times in the region 49 to 600 μs after muon injection was considered. The pileup contribution to the spectrum was determined from the data and corrected for as in Ref. [3]. The effects of horizontal CBO were incorporated as modulations of the observed number of counts and asymmetry, whereas the modulation of the observed phase was neglected in the fitting function. The CBO modulation envelope was determined by partial Fourier integration and confirmed from the modulation of the observed average energies for equal phases of the $(g - 2)$ oscillation. The time dilated muon lifetime $\gamma\tau$ was fixed to the expected value. The treatment of muon losses followed the one described above. Slowly vanishing distortions of the positron spectra were parametrized empirically and were included in the fitting function to improve the overall quality of fit. Their correlation with the fitted frequency ω_a is weak.

In the third analysis, as in the second analysis, ω_a was determined from a multiparameter fit to the summed time spectrum of positrons detected with all calorimeters. Alternative methods were used to assess systematic uncertainties. In particular, to study the systematics associated with CBO, the data were strobed at fixed phases of the horizontal CBO modulation. Since $\omega_{\text{CBO,h}} > 2 \times \omega_a$, the $(g - 2)$ signal can be fully determined from the resulting spectra. Equation (2) was fitted to the spectra after strobing, giving a result for ω_a which is less sensitive by a factor of about 3 to CBO modulations of the asymmetry and phase than results from fits to the unstrobed spectrum.

In the fourth analysis the ratio introduced in Eq. (6) of Ref. [3], $r(t) \sim A(E) \sin[\omega_a t + \phi_a(E)]$, was fitted. The ratio is largely insensitive to changes of observed counts on time scales larger than $\tau_a = 2\pi/\omega_a \sim 4 \mu\text{s}$. The effects of asymmetry and phase modulation were not explicitly included in the fitting function. This analysis used summed calorimeter spectra, in which the asymmetry and phase modulation effects are suppressed by an order of magnitude as compared to summed results from fits to individual calorimeter spectra. The suppression originates in the symmetry of the experiment design and has been studied extensively by including the effects in the fits, by determining the energy modulation, and by Monte Carlo simulations.

The internal consistency of the results was verified in various ways. For all analyses the fitted frequency ω_a was found constant with the fit start time, up to statistical fluctuations. The Fourier transform of residuals from fits incorporating asymmetry and phase modulation exhibits none of the CBO related interference structure in Fig. 2. Figure 3(a) shows the results for fits to the spectra from individual detectors from the analysis described first. Figure 3(b) shows the results on ω_a versus positron energy.

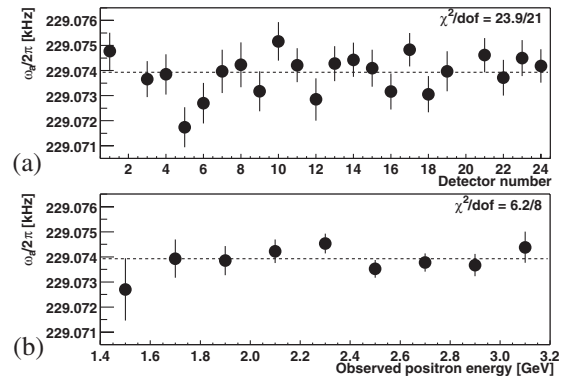


FIG. 3. (a) The frequency $\omega_a/(2\pi)$ determined from fits to the individual calorimeter time spectra. Data from calorimeters 2 and 20 were discarded, as in the analysis of our 1999 data. (b) The fitted frequency $\omega_a/(2\pi)$ versus positron energy. These results come from the analysis described first in the text.

The results from the analyses are found to agree, on ω_a to within 0.4 ppm. This is within the statistical variation of 0.5 ppm expected from the use of slightly different data selections and the different treatment of the data in the respective analyses. Each of the analyses gives results with comparable total uncertainties in ω_a . The analysis which incorporates asymmetry and phase modulation in the fitted function results in the smallest systematic uncertainty, primarily since CBO related systematic uncertainties are at the level of 0.05 ppm in this approach. The tradeoff is a slightly enlarged statistical uncertainty, since more CBO related parameters are fitted. The systematic uncertainty due to CBO is larger than our 1999 estimate [3] which did not include the effects from asymmetry and phase modulation. Neither the 1999 value of a_μ nor its total uncertainty were changed by this improved estimate. Other uncertainties are comparable or smaller.

We combine the present results to $\omega_a/(2\pi) = 229074.11(14)(7)$ Hz (0.7 ppm), which includes a correction of +0.76(3) ppm for contributions to Eq. (1) caused by vertical oscillations and, for muons with $\gamma \neq 29.3$, by horizontal electric fields. The stated uncertainties account

TABLE II. Systematic uncertainties for the ω_a analysis.

Source of errors	Size (ppm)
Coherent betatron oscillations	0.21
Pileup	0.13
Gain changes	0.13
Lost muons	0.10
Binning and fitting procedure	0.06
Others ^a	0.06
Total systematic error on ω_a	0.31

^aAGS background, timing shifts, E field and vertical oscillations, beam debunching/randomization.

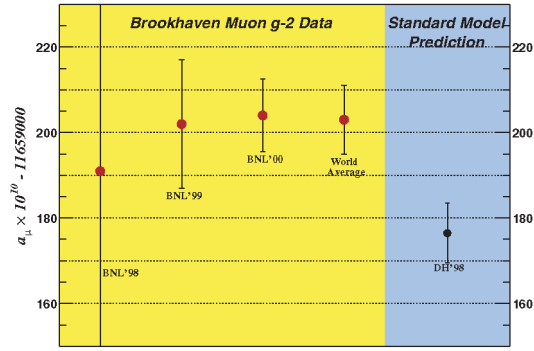


FIG. 4 (color online). Recent measurements of a_μ , together with the standard model prediction using the evaluation in Ref. [9] of $a_\mu(\text{had},1)$ from e^+e^- and τ decay data.

for strong correlations among the individual results, both statistical and systematic. Table II lists the systematic uncertainties in the combined result with these correlations taken into account.

After the ω_p and ω_a analyses were finalized separately and independently, a_μ was evaluated. The result is

$$a_{\mu^+} = \frac{R}{\lambda - R} = 11\,659\,204(7)(5) \times 10^{-10} \quad (0.7 \text{ ppm}), \quad (4)$$

in which $R = \omega_a/\omega_p$ and $\lambda = \mu_\mu/\mu_p = 3.183\,345\,39(10)$ [5]. This new result is in good agreement with previous measurements [1–3,6] and reduces the combined uncertainty by about half. The present world average experimental value is

$$a_\mu(\text{exp}) = 11\,659\,203(8) \times 10^{-10} \quad (0.7 \text{ ppm}), \quad (5)$$

which is driven by our determinations of a_μ in Refs. [2,3] and Eq. (4), and accounts for correlations between systematic uncertainties.

The theoretical value of a_μ in the standard model (SM) is determined from $a_\mu(\text{SM}) = a_\mu(\text{QED}) + a_\mu(\text{had}) + a_\mu(\text{weak})$, in which $a_\mu(\text{QED}) = 11\,658\,470.57(0.29) \times 10^{-10}$ (0.025 ppm) [7] and $a_\mu(\text{weak}) = 15.1(0.4) \times 10^{-10}$ (0.03 ppm) [8]. The hadronic contribution $a_\mu(\text{had})$ receives its leading contribution from $a_\mu(\text{had},1)$, which is currently evaluated to be $a_\mu(\text{had},1) = 692(6) \times 10^{-10}$ (0.6 ppm) [9]. The two more recent, published evaluations [10,11] used recent, preliminary data from Novosibirsk which have since been superseded [12], so we choose not to use their values for comparison. Higher order contributions include $a_\mu(\text{had},2) = -10.0(0.6) \times 10^{-10}$ [13] and the contribution from hadronic light-by-light scattering, which we now take to be $a_\mu(\text{had},\text{lbl}) = 8.6(3.2) \times 10^{-10}$ [14]. The chiral perturbation calculation of Ref. [15] provides an estimate with larger uncertainty. Hence, the value of $a_\mu(\text{SM})$ is currently evaluated to be

$$a_\mu(\text{SM}) = 11\,659\,177(7) \times 10^{-10} \quad (0.6 \text{ ppm}). \quad (6)$$

Additional data on e^+e^- collisions [12,16] and on τ decay [17] have been published and are being considered in future evaluations of $a_\mu(\text{had},1)$. New data can be expected from the Frascati ϕ factory and from the B factories.

The three most recent measurements of a_μ along with the above standard model prediction are shown in Fig. 4. The present experimental uncertainty is about half the size of the weak contribution to $a_\mu(\text{SM})$. The difference of $a_\mu(\text{expt})$ and $a_\mu(\text{SM})$ is about 2.6 times the combined experimental and stated theoretical uncertainty.

In 2001 data on μ^- were obtained. Approximately 3×10^9 decay electrons were observed. Field focusing indices $n = 0.122$ and $n = 0.142$ were used. Measurement of a_{μ^-} will provide a sensitive test of CPT violation and also an improved value of a_μ . We plan further data taking with μ^- to obtain an additional 6×10^9 counts.

We thank T. Kirk, D. I. Lowenstein, P. Pile, and the staff of the BNL AGS for the strong support they have given this experiment. We thank J. Bijnens, A. Czarnecki, M. Davier, S. I. Eidelman, A. Höcker, F. Jegerlehner, T. Kinoshita, W. Marciano, and E. de Rafael for helpful discussions. This work was supported in part by the U.S. Department of Energy, the U.S. National Science Foundation, the U.S. National Computational Science Alliance, the German Bundesminister für Bildung und Forschung, the Russian Ministry of Science, and the U.S.-Japan Agreement in High Energy Physics.

-
- [1] R. M. Carey *et al.*, Phys. Rev. Lett. **82**, 1632 (1999).
 - [2] H. N. Brown *et al.*, Phys. Rev. D **62**, 091101 (2000).
 - [3] H. N. Brown *et al.*, Phys. Rev. Lett. **86**, 2227 (2001).
 - [4] A. Yamamoto *et al.*, Nucl. Instrum. Methods Phys. Res., Sect. A (to be published); G. T. Danby *et al.*, Nucl. Instrum. Methods Phys. Res., Sect. A **457**, 151 (2001); E. Efstathiadis *et al.*, Nucl. Instrum. Methods Phys. Res., Sect. A (to be published); R. Prigl *et al.*, Nucl. Instrum. Methods Phys. Res., Sect. A **374**, 118 (1996); X. Fei, V. Hughes, and R. Prigl, Nucl. Instrum. Methods Phys. Res., Sect. A **394**, 349 (1997); S. A. Sedykh *et al.*, Nucl. Instrum. Methods Phys. Res., Sect. A **455**, 346 (2000).
 - [5] W. Liu *et al.*, Phys. Rev. Lett. **82**, 711 (1999); D. E. Groom *et al.*, Eur. Phys. J. C **15**, 1 (2000).
 - [6] J. Bailey *et al.*, Nucl. Phys. **B150**, 1 (1979).
 - [7] P. Mohr and B. Taylor, Rev. Mod. Phys. **72**, 351 (2000), and references therein.
 - [8] A. Czarnecki and W. J. Marciano, Phys. Rev. D **64**, 013014 (2001).
 - [9] M. Davier and A. Höcker, Phys. Lett. B **435**, 427 (1998).
 - [10] S. Narison, Phys. Lett. B **513**, 53 (2001).
 - [11] J. F. de Trocóniz and F. J. Ynduráin, Phys. Rev. D **65**, 093001 (2002).
 - [12] R. R. Akhmetshin *et al.*, Phys. Lett. B **527**, 161 (2002).
 - [13] B. Krause, Phys. Lett. B **390**, 392 (1997); R. Alemany, M. Davier, and A. Höcker, Eur. Phys. J. C **2**, 123 (1998).

-
- [14] M. Knecht, A. Nyffeler, M. Perrottet, and E. de Rafael, Phys. Rev. Lett. **88**, 071802 (2002); M. Knecht and A. Nyffeler, Phys. Rev. D **65**, 073034 (2002); M. Hayakawa and T. Kinoshita, hep-ph/0112102; J. Bijnens, E. Pallante, and J. Prades, Nucl. Phys. **B626**, 410 (2002); I. Blokland, A. Czarnecki, and K. Melnikov, Phys. Rev. Lett. **88**, 071803 (2002).
- [15] M. Ramsey-Musolf and M. B. Wise, Phys. Rev. Lett. **89**, 041601 (2002).
- [16] Z.-G. Zhao, Int. J. Mod. Phys. A **15**, 3739 (2000); J. Z. Bai *et al.*, Phys. Rev. Lett. **84**, 594 (2000); **88**, 101802 (2002).
- [17] S. Anderson *et al.*, Phys. Rev. D **61**, 112002 (2000).